# Optical absorption spectra of the one-dimensional ferromagnet $CsFeCl_3$

Taiju Tsuboi
*Physics Department, Kyoto Sangyo University, Kamigamo, Kyoto 603, Japan*

Meiro Chiba
*Institute of Atomic Energy, Kyoto University, Uji, Kyoto 611, Japan*

Yoshitami Ajiro
*Department of Chemistry, Kyoto University, Kyoto 606, Japan*
(Received 17 January 1985)

Polarized absorption spectra of the one-dimensional (1D) ferromagnet $CsFeCl_3$ have been investigated from 3000 to 400 nm from 15 to 295 K. Several weak bands are seen at the low-energy sides of the $C$, $E$, and $F$ bands, whose temperature dependence of intensity agrees with that predicted for the 1D ferromagnet: This is the first observation of hot magnon sideband in $CsFeCl_3$. It turns out that (1) the parity-forbidden but spin-allowed $A$ band arises not only from the vibration-assisted electric dipole transition but also from the magnetic dipole transition and (2) the parity- and spin-forbidden $B-F$ bands arise not only from the intrachain ferromagnetic spin-exchange-induced electric dipole transition in two adjacent $Fe^{2+}$ ions, giving rise to hot magnon sidebands, but also from the magnetic dipole transition in a single $Fe^{2+}$ ion. All the $A-G$ absorption bands are attributed to the $Fe^{2+}$ crystal-field energy state of the $d^6$ electronic configuration. It is revealed by a computer analysis that an absorption band attributable to the $^3T_{2g}(^3F)$ state is obscured by the sharply structured $E$ and $F$ bands.

## I. INTRODUCTION

A number of studies have been done on the optical properties of magnetic materials, especially the optical detections of the magnetic phase transition, short-range or long-range spin ordering, and magnon and exciton migrations. Most of the work has been carried out on two- or three-dimensional antiferromagnets. Of the various magnetic insulators, the one-dimensional (1D) or linear-chain ferromagnet has not been widely studied, presumably because examples of 1D ferromagnets are exceedingly rare and it is difficult to grow the crystals. So far, optical absorption measurements have been done on $CsNiF_3$,[1-4] $CsFeCl_3$,[5,6] $RbFeCl_3$,[5-7] and $KFeCl_3$.[6] These insulators are, strictly speaking, not purely 1D ferromagnets since an inevitable interchain magnetic coupling exists, but they can be identified as quasi-1D ferromagnets since a strong short-range ferromagnetic ordering exists along the chain. An excellent review of the ferromagnetism in such linear chain compounds has been given by Willett, Gaura, and Landee.[8]

A current topic of interest in 1D ferromagnets is the "hot" magnon sideband (called hot band hereafter) which is expected to exhibit different features from a 2D or 3D ferromagnet or antiferromagnet, e.g., on the temperature dependence of the intensity.[6,9,10] In antiferromagnets both hot and cold bands are allowed, whereas in ferromagnets only the hot band is allowed.[11] In the 1D antiferromagnet, the hot band has not been observed yet although the cold band was found only in $CsMnCl_3 \cdot 2H_2O$ by Jia, Strauss, and Yen.[12] On the other hand, in the 1D ferromagnet the hot band was observed in $CsNiF_3$ (Ref. 1) and $KFeCl_3$ (Ref. 6). An unusual temperature dependence with a large residual intensity at 0 K has been obtained for all the absorption bands in $CsFeCl_3$ (Ref. 6) and $RbFeCl_3$ (Refs. 6 and 7), which is different from a theoretical temperature dependence calculated by Ebara and Tanabe for the hot band in 1D ferromagnet.[10] Is the hot band present in $CsFeCl_3$ and $RbFeCl_3$? Is it true that the reason why the usual hot band was observed in $KFeCl_3$ but not in $RbFeCl_3$ and $CsFeCl_3$ arises from the difference of crystal structure ($KFeCl_3$ has orthorhombic $D_{2h}^{16}$ symmetry, whereas $RbFeCl_3$ and $CsFeCl_3$ hexagonal $D_{6h}^4$ symmetry)? The present work was undertaken to clarify whether the hot band appears in $CsFeCl_3$ or not. For that purpose, we investigate the temperature dependence of the absorption spectrum in detail. $CsFeCl_3$ was selected because its one dimensionality is better than $RbFeCl_3$,[13] although both crystals show unexpectedly poor one dimensionality.[13,14]

In addition to the above-mentioned questions, more questions arose while reading the recent literature reporting the absorption spectra of $CsFeCl_3$. For example, the absorption spectra obtained by Putnik *et al.*[5] are not in agreement with those by Krausz *et al.*[6] with respect to the $\sigma(E||c)$ polarized spectrum. Which spectrum is correct? Secondly, the large absorption band appearing at about 7300 $cm^{-1}$ exhibits a strong temperature dependence, indicating that the band is due to the spin-allowed $^5T_{2g} \rightarrow {}^5E_g$ transition whose intensity can be enhanced by the phonon coupling. What kind of lattice vibration does couple to the $^5E_g$ state? Is the infrared band caused only by such a vibration-assisted transition? In this paper we try to answer these questions in order to understand the absorption spectra of $CsFeCl_3$.

 

## II. EXPERIMENTAL PROCEDURE AND RESULTS

Polarized absorption spectra in the visible through infrared region were measured with a Shimadzu MPS-50L spectrophotometer. A Glan prism was used as a polarizer. The crystal used for the measurement has dimensions of about $8\times5\times0.6$ mm$^3$, which was cut along the crystal $c$ axis. Single crystals of $CsFeCl_3$ were grown using the Bridgeman method by Dr. K. Adachi. The crystal was cooled in an Osaka Sanso Crio-Mini cryostat which allows cooling down to 15 K.

Figure 1 shows the $\sigma$- and $\pi$-polarized absorption spectra of $CsFeCl_3$ at 15 K. The $\sigma$ and $\pi$ spectra were obtained using the polarized light of electric vector parallel and perpendicular to the $c$ axis, respectively. All the broadbands except a band peaking at 820 nm are larger in the $\sigma$ spectrum than in the $\pi$ spectrum. The same is true for all temperatures between 15 and 300 K measured. No difference is found between the $\sigma$ and $\pi$ spectra except the band intensity. Putnik *et al.*,[5] however, observed several bands in the $\sigma$ spectrum which are not observed in the $\pi$ spectrum, e.g., two sharp bands peaking at 19 186 and 19 410 cm$^{-1}$. From the agreement of the spectra of Krausz *et al.* with ours, it is concluded that these additional bands are not attributed to $Fe^{2+}$. We call the observed bands $A,B,\ldots,H$ bands in order of increasing energy as indicated in Fig. 1. Of these bands, the $G$ band consists of two sharp bands with peaks at 426.5 and 429.0 nm. The other $A$, $B$, $C$, $D$, $E$, $F$, and $H$ bands have peaks at 1360, 820, 657, 545, 494.4, 472, and 415 nm, respectively. Fine structure is observed in the $C$ band at the low-energy side (Fig. 2) and in the sharp $E$ and $F$ bands at their low-energy tails (Fig. 3). These sidebands are observed not only at 15 K but also at high temperatures such as 100 K.

It is difficult to obtain the temperature dependence of the intensity (i.e., area) of absorption band exactly since the overlap between the bands is strong at high temperatures as seen in Fig. 3. The $A$ and $\sigma$-polarized $C$ bands, however, are well isolated from other bands (see Figs. 2 and 4), so that we can estimate their intensities easily and precisely. They are plotted in Figs. 5 and 6. The $A$-band intensity $f$ is constant at low temperatures but increases in proportion to $T$ at high temperatures. The behavior is similar to the case of the vibration-assisted transition described by $f(T)=f(0)\coth(h\nu/2k_BT)$, where $\nu$ is the frequency of lattice vibration, $h$ the Planck constant, and $k_B$ the Boltzmann constant.[15] Precisely speaking, the os-

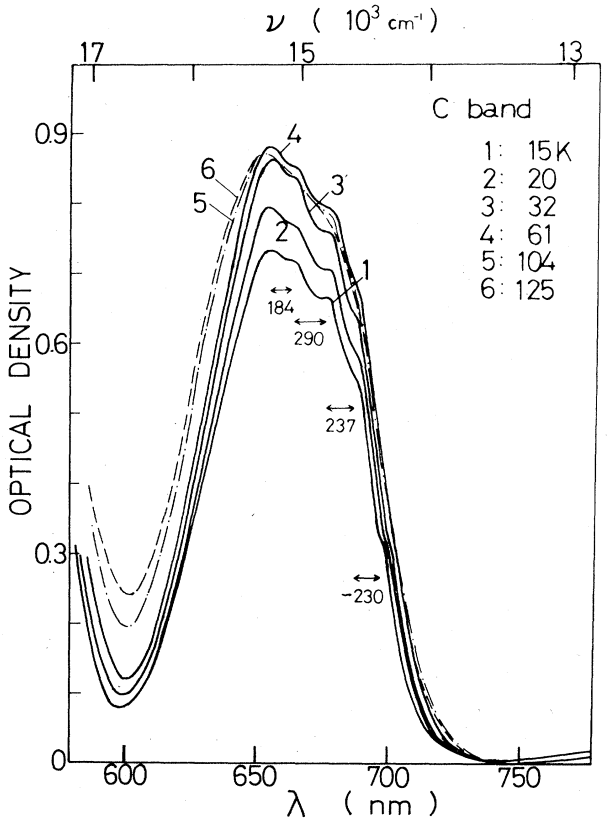


FIG. 2. The $\sigma$-polarized absorption spectra of the $C$ band at various temperatures. The spacing between the sidebands is indicated in units of cm$^{-1}$.

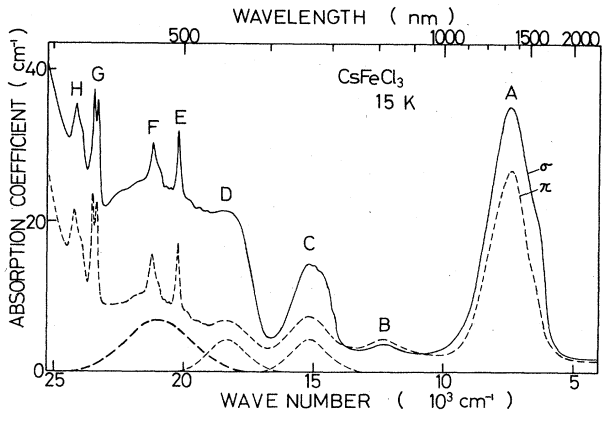


FIG. 1. The $\sigma(E||c)$ and $\pi(E\perp c)$ polarized absorption spectra of $CsFeCl_3$ at 15 K. At the bottom are shown the decomposed $C$ and $D$ bands and a new band hidden under the $E$ and $F$ bands, which are obtained from the $\pi$ spectrum (see text).

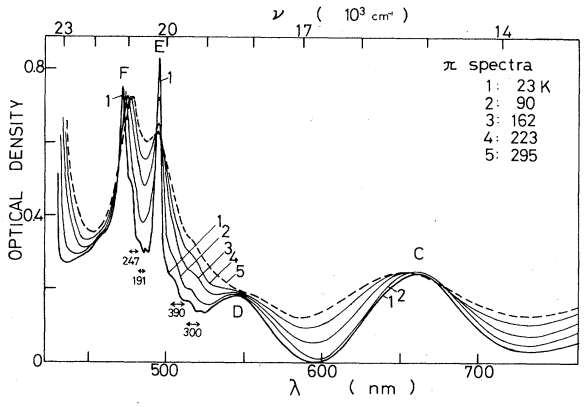


FIG. 3. The $\pi$-polarized absorption spectra in the $C$-, $D$-, $E$-, and $F$-band regions at various temperatures. The spacing between the sidebands is indicated in units of cm$^{-1}$.

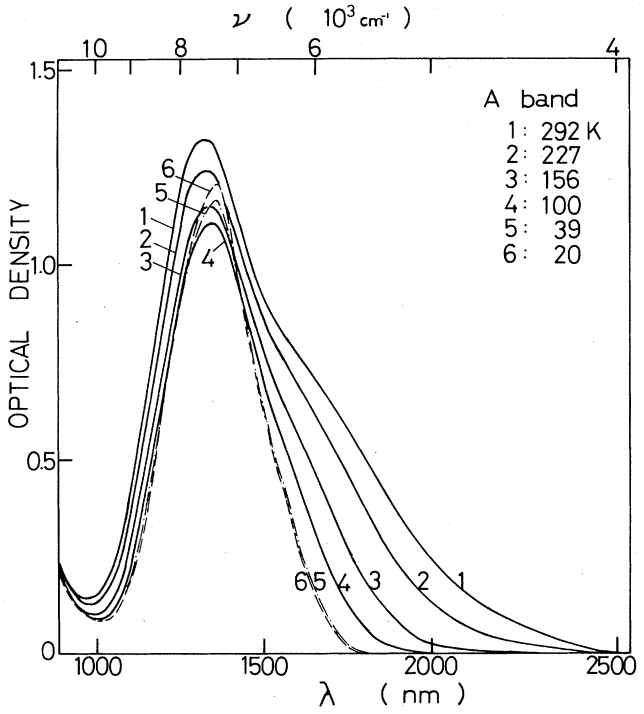


FIG. 4. The $\pi$-polarized absorption spectra of the $A$ band at various temperatures.

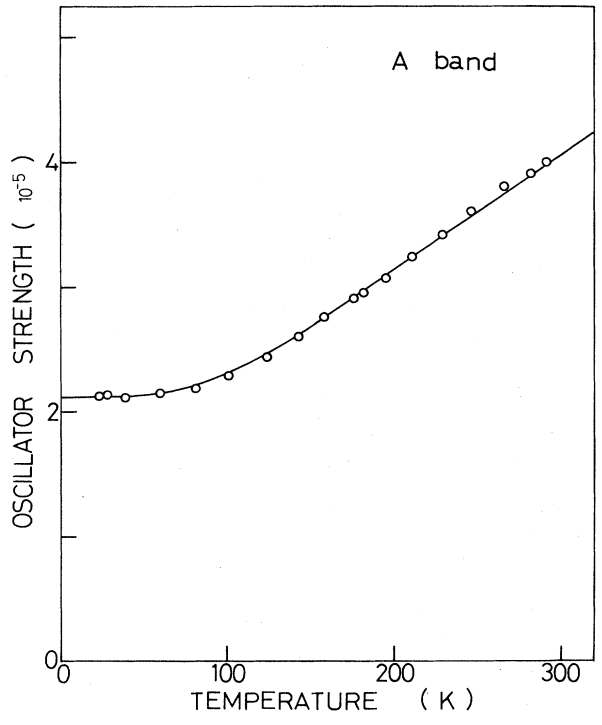


FIG. 5. Absorption intensity of the $\pi$-polarized $A$ band plotted against temperature. The solid curve is $f(T)=f_0+f(0)\coth(h\nu/k_BT)$ with $f_0=0.75\times10^{-5}$, $f(0)=1.37\times10^{-5}$, and $\nu=185$ cm$^{-1}$.

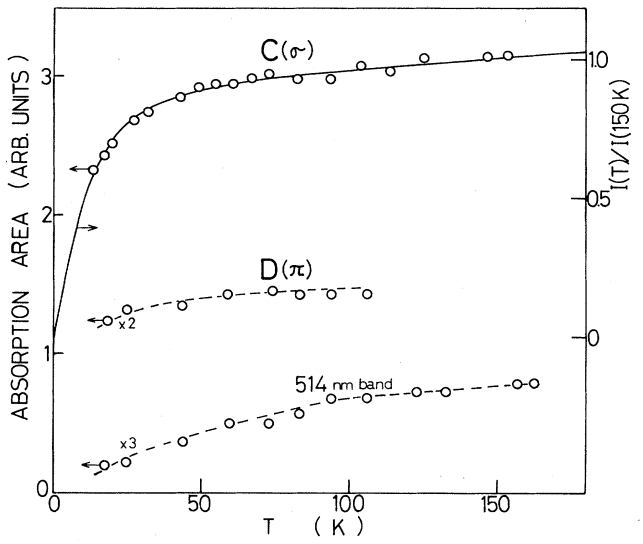


FIG. 6. Absorption intensity (area) of the $\sigma$-polarized $C$ band, $\pi$-polarized $D$, and 514-nm bands plotted against temperature. The solid curve (scale on right) shows a theoretical temperature dependence calculated using Ebara and Tanabe theory (see text).

cillator strength of the $A$ band can be described by $f(T)=f_0+f_1(0)\coth(h\nu/2k_BT)$ with $f_0=0.75\times10^{-5}$, $f_1(0)=1.37\times10^{-5}$, and $\nu=185$ cm$^{-1}$. On the other hand, the $C$-band intensity increases rapidly with increasing temperature in the low-temperature region, and above 50 K it increases slowly as seen in Fig. 6.

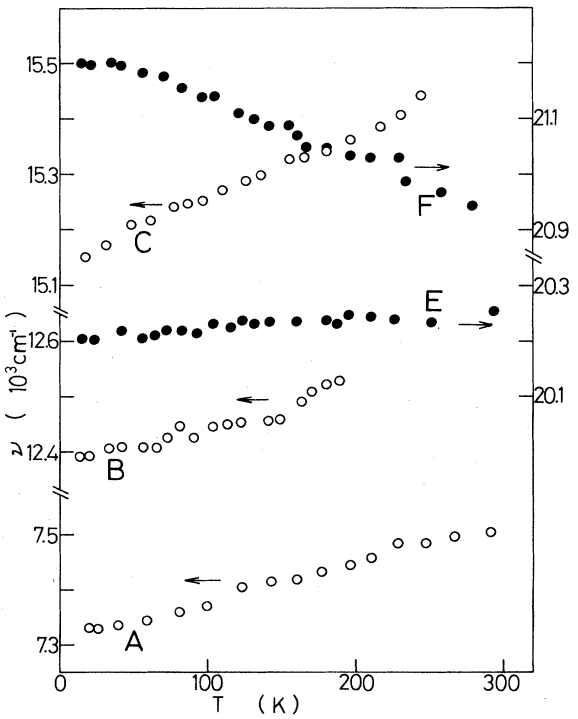


FIG. 7. Peak position of the $A$, $B$, $C$, $E$, and $F$ bands plotted against temperature. For the $E$ and $F$ bands the scale is on the right.

We tried to obtain the intensity of other bands, although there were difficulties in choosing their baselines. In Fig. 6 are plotted the intensities of the broad $D$ band and of a weak band peaking at 514 nm which appears as the sideband of the sharp $E$ band. The $D$ band apparently exhibits a temperature dependence quite similar to the $C$ band. To obtain reliable values for these bands, i.e., to avoid the ambiguity in choosing the baseline, we do not compare the spectra measured at 15 K and any temperature, but we estimate the difference between spectra at two temperatures that are close to each other, since the two spectra have almost the same baseline.

Figure 7 shows the temperature dependence of peak positions of various absorption bands. The $E$ band shifts toward the high-energy side with increasing temperature as do the $A$, $B$, and $C$ bands although the amount is smaller than the cases of the latter bands, whereas only the $F$ band shifts toward the low-energy side. The $E$ and $F$ bands are located close to each other; their separation is 1000 $cm^{-1}$ at 20 K. As seen in Fig. 4, the $A$ band consists of two bands which are split by the Jahn-Teller effect on the $^5E_g$ state.[6,16] The separation is about 1000 $cm^{-1}$, the same as the $E$-$F$ band separation. Unlike the case of the dynamic Jahn-Teller effect, however, the $E$-$F$ band separation decreases with increasing temperature as seen in Fig. 7. This indicates that the $E$ and $F$ band separation is not caused by Jahn-Teller effect.

## III. DISCUSSION

### A. Spin-allowed band

The temperature dependence of the $A$ band intensity is quite similar to the case of parity-forbidden but spin-allowed transition bands.[17] Thus the $A$ band that is attributed to the $^5T_{2g}\rightarrow{}^5E_g$ transition is confirmed to be due to a vibration-assisted transition. The frequency of the lattice vibration involved was estimated to be $\nu=185$ $cm^{-1}$ as mentioned above. This value is quite close to the frequency 186 $cm^{-1}$ of the $A_{2u}$ vibrational mode in $CsFeCl_3$.[18] This indicates that the odd-parity vibration certainly plays an important role in relaxing the parity selection rule. Presumably, it induces a mixing of the high-energy $^5A_{2u}$ state of the $d^5p$ odd-parity electron configuration of $Fe^{2+}$ into the $^5E_g$ state of $d^6$ configuration, making the $^5T_{2g}\rightarrow{}^5E_g$ transition electric-dipole allowed. In addition to such a vibronic contribution $f_1(0)\coth(h\nu/2k_BT)$, the $A$ band intensity $f(T)$ has a constant term $f_0$. What gives rise to the $f_0$ value for the $A$ band? The $^5T_{2g}\rightarrow{}^5E_g$ transition is electric dipole forbidden, but it is magnetic-dipole allowed. Generally speaking, the magnetic-dipole-allowed band has a value of oscillator strength $f=\sim10^{-5}$–$10^{-6}$.[15] This value is close to our $f_0=0.75\times10^{-5}$.

Besides the magnetic-dipole process in single $Fe^{2+}$ ion, the intrachain spin-exchange process within two adjacent $Fe^{2+}$ ions is conceivable as the origin of the $f_0$ value. This process gives rise to the temperature-dependent hot band, the intensity of which approaches zero at 0 K. A finite value would be obtained for the absorption intensity at 0 K if we took into account the interchain antiferromagnetic exchange interaction in the two neighboring $Fe^{2+}$ ions. The latter interaction, however, is considerably weaker than the ferromagnetic interaction,[13] so that the $f_0=0.75\times10^{-5}$ value is not believed to be derived from the antiferromagnetic coupling. Furthermore, the latter process gives a temperature-dependent intensity which increases with increasing temperature from 0 K as seen in the 1D antiferromagnetic $N(CH_3)_4MnCl_3$ (TMMC).[19] Therefore it is concluded that the temperature-independent $f_0$ value is predominantly due to the magnetic dipole transition.

### B. Level assignment for the spin-forbidden bands

A comparison of the absorption spectrum with the crystal-field energy-level diagram[6] suggests that the $A$, $B$, and $C$ bands are attributable to the transition from the ground state $^5T_{2g}$ to $^5E_g$ ($^5D$ state of free $Fe^{2+}$), $^3T_{1g}(^3P)$, and $^3T_{1g}(^3H)$ states in cubic $Fe^{2+}$, respectively. Similarly, two peaks of the $G$ band are attributable to $^3A_{2g}(^3F)$ and $^3T_{2g}(^3G)$ states in order of increasing energy. On the other hand, it has been suggested that the $D$ band arises from double-exciton band of the $(^5T_{2g}+{}^5T_{2g})\rightarrow(^5E_g+{}^5E_g)$ transition or charge-transfer band.[6] If it arises from the double excitation, its intensity should decrease monotonically with increasing temperature as observed in the ferromagnet $CsNiF_3$ (Refs. 1 and 3) and various antiferromagnets.[20] The $D$ band never shows such a temperature dependence as seen in Fig. 6. Furthermore the $D$-band peak position ($\sim18\,350$ $cm^{-1}$) deviates considerably from the expected position $2\times7330$ $cm^{-1}$, where 7330 $cm^{-1}$ is the $A$-band peak position. Therefore, we cannot assign the $D$ band to the double exciton band. It is probable to assign it to a single-exciton band as with the case of other bands since (1) its temperature dependence is similar to the $C$ band and (2) the crystal-field-level diagram[6] indicates that the $D$ band corresponds to the $^3T_{2g}(^3H)$ level.

Krausz *et al.* did not assign the $D$ band to the $^3T_{2g}$ level because it is intense and extraordinarily broad (according to them, the half-width is 5000 $cm^{-1}$ at 5 K).[6] The $\pi$-polarized $D$ band, however, has a half-width of 1480 $cm^{-1}$ at 18 K, which is almost the same as the $C$ band, and its intensity is 0.77 times of the $C$ band. This indicates that the $D$ band is not as broad and intense compared with other bands. It seems natural to assign the $D$ band to the $^3T_{2g}$ state since all the other crystal field levels correspond to the observed bands quite well (see below and Fig. 3 of Ref. 6). The $D$ band certainly becomes strong in the $\sigma$ spectrum, as Krausz *et al.* have suggested. We note, however, that such a strong dichroism is observed not only for the $D$ band but for the $A$ and $C$ bands as well.

According to the crystal-field calculation,[6] three levels of $^3T_{1g}$ ($^3H$), $^3T_{2g}(^3F)$, and $^3E_g(^3H)$ are located in the (20 000–21 000)-$cm^{-1}$ region where $E$ and $F$ bands are observed. To which levels are the $E$ and $F$ bands attributable? We note the following three points: (1) The $^3E_g$ state is located at a higher energy than the $^3T_{1g}$ state by about 1000 $cm^{-1}$, (2) the $^3T_{1g}$-level position is quite close to the $E$ band, and (3) the two levels arise from the same $^3H_2$ state of free $Fe^{2+}$, whereas the $^3T_{2g}$ level arises from

the $^3F$ state. Therefore, taking into account that the $E$ and $F$ bands have similar sharp peaks, we will be allowed to attribute these bands to the $^3T_{1g}$ and $^3E_g$ levels, respectively. Where is the absorption band that is attributable to the remaining $^3T_{2g}(^3F)$ level?

When we closely look at the absorption spectra in the (20 000—22 000)-cm$^{-1}$ region, we find that a broad band seems to be present under the $E$ and $F$ bands. Using a computer analysis, we revealed a Gaussian-shaped broad band which is similar to the $C$ and $D$ bands. In this analysis, we assumed a symmetric band shape for the sharp $E$ and $F$ bands and for the broad $\pi$-polarized $C$ and $D$ bands, and we subtracted these bands and the low-energy tail of the $G$ band from the observed $\pi$ spectrum. As shown in the bottom of Fig. 1, the new band has a peak at about 21 000 cm$^{-1}$ and a half-width of about 2800 cm$^{-1}$. The energy-level calculation suggests that the $^3T_{2g}(^3F)$ level position is between the $^3T_{1g}(^3H)$ and $^3E_g(^3H)$ level positions.[6] This is consistent with the peak position of the new band.

### C. Magnon sideband

The sidebands are observed on the low-energy side of the $C$, $E$, and $F$ bands as seen in Figs. 2 and 3. We may propose two possibilities as the origin of the sidebands: one is the phonon sidebands and the other is magnon sidebands. According to the infrared spectrum measurement,[18] phonon absorption bands appear at 245, 186, 158, 76, and 52 cm$^{-1}$ for $CsFeCl_3$, which correspond to the frequencies of $E_{1u}(a)$, $A_{2u}(a)$, $E_{1u}(b)$, $E_{1u}(c)$, and $A_{2u}(b)$ modes, respectively. Unlike the case of vibrational structure,[21] the spacings between the neighboring peaks in the $C$ band are not equal (Fig. 2), so that we cannot determine which vibrational mode is responsible for the fine structure. The same is true for the fine structure of the $E$ and $F$ bands. In addition to such a fact that there is no simple progression corresponding to the vibrational mode, the sidebands exist even at high temperatures above 100 K, i.e., the fine structure at 15 K can be even found at 100 K. It is usually observed that the phonon sidebands are rapidly broadened and their peak height is reduced as temperature is increased, resulting in a disappearance of phonon structure at high temperatures like 100 K. Therefore, our fine structures are not attributable to phonon sidebands.

When the temperature is raised from 15 K, these sidebands are observed to increase remarkably as seen in Figs. 2 and 3. At the bottom of Fig. 6 is shown the temperature dependence of a weak sideband peaking at 514 nm. Since the same temperature dependence was obtained for other sidebands associated with $C$ and $F$ bands, all sidebands in $CsFeCl_3$ are suggested to arise from the same origin. In $KFeCl_3$ Krausz *et al.* observed strongly temperature-dependent, weak bands at 19 400 cm$^{-1}$ (515.5 nm) and 23 490 cm$^{-1}$ (425.7 nm); these bands have been assigned to hot bands since they grow with increasing temperature.[6] Our sideband peaking at 514 nm is close to the 515.5-nm band position of $KFeCl_3$ and has an asymmetric line shape with a broadness at the low-energy side similar to the 515.5-nm band. Additionally, as in the case of the 515.5-nm band, the 514-nm band of $CsFeCl_3$ exhibits the temperature dependence predicted theoretically for the 1D ferromagnet.[10] Thus, it is concluded that the 514-nm band of $CsFeCl_3$ and therefore other sidebands of the $C$ and $F$ bands are attributable to the hot band.[22]

Let us investigate in detail whether the above conclusion is certainly true for the sideband of the $C$ band or not. We calculated the temperature dependence of the hot-band intensity for $CsFeCl_3$ (spin $S=2$, intrachain ferromagnetic exchange energy[13] $J=1.83$ cm$^{-1}$) using the Ebara and Tanabe theory.[10] The theoretical intensity $I(T)/I(150\text{ K})$ is compared with the measured $C$-band intensity in Fig. 6, where we adjusted the scale of $I(T)/I(150\text{ K})$ to fit the theoretical curve into the experiment as well as possible. It is noted that good agreement was obtained between the theoretical curve and experiment. This indicates that the temperature-dependent part of the $C$-band intensity certainly arises from the hot bands.

The theoretical curve of Fig. 6 never approaches zero but approaches a finite intensity $f'_0$ at 0 K, about one-half of the intensity at 15 K. A similar temperature dependence has been observed for the other broad $B$ and $D$ bands and even for the sharp $E$ and $F$ bands.[6] This can be interpreted as follows: Each of these bands does not consist of only the hot bands but it contains additional non-hot-magnon bands such as pure exciton bands, giving rise to the residual intensity at 0 K. Unlike the $C$ bands, the sidebands are not observed in the $B$ and $D$ bands. It is believed in these bands that magnon sidebands are not sufficiently resolved to be distinguished from one another, the same as the broad bands observed in various magnetic insulators. What gives the intensity to the non-hot-magnon part in these spin-forbidden bands? It seems that the magnetic-dipole process plays an important role as the case of the $A$ band. Unlike the case of the spin-allowed $A$ band, however, the spin-orbit interaction is necessary to make these spin-forbidden transitions magnetic-dipole allowed. Therefore the residual oscillator strength $f'_0$ of the spin-forbidden band is expected to be smaller than the $f_0$ value of the $A$ band. This is consistent with the estimation that the $f'_0$ value of the $\pi$-polarized $C$ band is about $\frac{1}{7}$ of the $f_0$ value.

## IV. CONCLUSIONS

The main conclusions from the absorption spectrum measurements described in this paper are the following.

(1) The $A$ band associated with the spin-allowed but parity-forbidden $^5T_{2g}\rightarrow{}^5E_g$ transition is due to (a) the magnetic dipole transition and (b) the electric dipole transition, which is induced by the coupling of lattice vibration with $A_{2u}$ odd-parity mode into the $^5E_g$ state.

(2) The strongly temperature-dependent fine structure is observed at the low-energy sides of the $C$, $E$, and $F$ bands. The temperature dependence is quite similar to the hot bands observed in the 1D ferromagnets $CsNiF_3$ and $KFeCl_3$. From the comparison with the Ebara and Tanabe theory, the fine structure is attributed to hot magnon sideband.

(3) The spin- and parity-forbidden bands are due to (a) the magnetic dipole transition in single $Fe^{2+}$ ion which is

accompanied with the spin-orbit interaction and (b) the electric dipole transition induced by the intrachain ferromagnetic exchange coupling in two adjacent $Fe^{2+}$ ions, giving rise to the hot bands.

(4) From the comparison with the crystal-field energy-level diagram for $Fe^{2+}$ and from the temperature dependence, the *A*, *B*, *C*, *D*, *E*, *F*, and *G* bands are attributed to the transition from the ${}^5T_{2g}$ ground state to the ${}^5E({}^5D)$, ${}^3T_{1g}({}^3P)$, ${}^3T_{1g}({}^3H)$, ${}^3T_{2g}({}^3H)$, ${}^3T_{1g}({}^3H)$, ${}^3E_g({}^3H)$, and ${}^3A_{2g}({}^3F)+{}^3T_{2g}({}^3G)$ states, respectively. The absorption band corresponding to the ${}^3T_{2g}({}^3F)$ state is revealed to be present at 21 000 $cm^{-1}$. There is no energy level corresponding to the *H* band in the diagram. From its peak position, it is temporarily suggested to the double exciton band due to the ${}^5T_{2g}+{}^5T_{2g}\rightarrow{}^3T_{1g}({}^3P)+{}^3T_{1g}({}^3P)$ transition. The details will be studied later.

(5) Unlike the other bands, the *F*-band peak is observed to exhibit a red shift with increasing temperature. The reason is an open question to us.

## ACKNOWLEDGMENTS

We wish to thank Professor Y. Tanabe and Dr. K. Ebara for giving us a detailed explanation of their theory on 1D ferromagnets, and to Dr. K. Adachi for growing $CsFeCl_3$ single crystals.

[1]E. Imppu, R. Laiho, T. Levola, and T. Tsuboi, Phys. Rev. B **30**, 232 (1984).

[2]T. Tsuboi and R. Laiho, Phys. Rev. B (to be published).

[3]R. H. Petit, J. Ferre, and J. Nouet, Physica **86-88B**, 1213 (1977).

[4]J. Cibert, Y. Merle d'Aubigne, J. Ferre, and M. Regis, J. Phys. C **13**, 2781 (1980).

[5]C. F. Putnik, G. Mattney Cole, B. B. Garret, and S. L. Hobt, Inorg. Chem. **15**, 826 (1976).

[6]E. Krausz, S. Viney, and P. Day, J. Phys. C **10**, 2685 (1977).

[7]N. Bontemps, C. Grisolia, M. Nozzi, and B. Briat, J. Appl. Phys. **53**, 2710 (1982).

[8]R. D. Willett, R. M. Gaura, and C. P. Landee, *Extended Linear Chain Compounds,* edited by J. S. Miller (Plenum, New York, 1983), Vol. 3, p. 143.

[9]T. Tsuboi, Phys. Lett. **102A**, 148 (1984); T. Tsuboi and W. Kleemann, Phys. Rev. B **27**, 3762 (1983).

[10]K. Ebara and Y. Tanabe, J. Phys. Soc. Jpn. **36**, 93 (1974); K. Ebara (private communication).

[11]See, e.g., D. J. Robbins and P. Day, J. Phys. C **9**, 867 (1976).

[12]W. Jia, E. Strauss, and W. M. Yen, Phys. Rev. B **23**, 6075 (1981).

[13]H. Yoshizawa, W. Kozukue, and K. Hirakawa, J. Phys. Soc. Jpn. **49**, 144 (1980).

[14]M. Steiner, K. Kakurai, W. Knop, B. Dorner, R. Pynn, U. Happek, P. Day, and G. McLeen, Solid State Commun. **38**, 1179 (1981).

[15]C. J. Ballhausen, *Introduction to Ligand Field Theory* (McGraw-Hill, New York, 1962), Chap. 8; S. Sugano, Y. Tanabe, and H. Kamimura, *Multiplets of Transition-Metal Ions in Crystals* (Academic, New York, 1970), Chap. 5.

[16]J. Ferguson, H. J. Guggenheim, and E. R. Krausz, Aust. J. Chem. **22**, 1909 (1969).

[17]J. Brynestad, H. Yakel, and G. P. Smith, J. Chem. Phys. **45**, 4562 (1966); J. Ferre, R. V. Pisarev, M. J. Harding, J. Badoz, and S. A. Kizhaev, J. Phys. C **6**, 1623 (1973).

[18]G. L. McPherson and J. R. Chang, Inorg. Chem. **12**, 1196 (1973).

[19]P. Day and L. Dubicki, J. Chem. Soc. Faraday Transact. II, **69**, 363 (1973); H. Yamamoto, D. S. McClure, C. Marzzaco, and M. Waldman, Chem. Phys. **22**, 79 (1977).

[20]See, e.g., F. J. Schäfer, W. Kleemann, and T. Tsuboi, J. Phys. C **16**, 3987 (1983); T. Fujiwara, W. Gebhardt, K. Petanides, and Y. Tanabe, J. Phys. Soc. Jpn. **33**, 39 (1972).

[21]See, e.g., R. V. Pisarev, J. Ferre, J. Duran, and J. Badoz, Solid State Commun. **11**, 913 (1972); W. Kleemann, F. J. Schaefer, and J. Nouet, J. Phys. C. **14**, 4447 (1981).

[22]The $d^6\rightarrow d^6$ transition spectra of various $Fe^{2+}$ compounds are quite similar to each other in regard to the peak positions and relative intensities (see, e.g., Refs. 5 and 6), just as the case of other transition-metal-ion compounds. Consequently, the absorption bands, which appear at almost same positions in the different $Fe^{2+}$ compounds, have been suggested to arise from the same origin.